Natural Hazards
https://doi.org/10.1007/s11069-025-07300-5

ORIGINAL PAPER

How do hydrogeological and socio-economic parameters influence the likelihood of NO_3^- pollution and Cl^- salinization? An application within the campania region (Italy)

Mojgan Bordbar[1] · Gianluigi Busico[1] · Stefania Stevenazzi[2] · Micòl Mastrocicco[1]

Received: 6 October 2024 / Accepted: 10 April 2025

Abstract

Groundwater pollution is increasing because of long-term human activities. This study aims at assessing the probability of nitrate (NO_3^-) and chloride (Cl^-) pollution. The approach firstly involved applying a Gaussian simulation to reconstruct the spatial distribution of the pollutants in three areas in the Campania Region (Italy). Then, probability maps were used to determine how different hydrogeological and socio-economic parameters affect groundwater quality in the three regions. To prioritize the factors affecting the target pollutions, two distinct groups of parameters were considered: hydraulic head, recharge, distance from inland water, distance from the coastline, ground elevation, hydraulic conductivity, and fine sediment content to assess Cl^- salinization; while hydraulic conductivity, recharge, fine sediment content, crops fertilizer request, depth to water table, and distance from wells to assess NO_3^- pollution. Three different algorithms, Decision Tree (DT), Random Forest (RF), and Information Gain Ratio (IGR), were employed. The results of the prioritization of parameters affecting NO_3^- pollution indicate that recharge, hydraulic conductivity, water depth, and crops fertilizer request are the most influential factors, while the results for Cl^- salinization show that hydraulic head, recharge, hydraulic conductivity, distance from inland water, and fine sediment content have the strongest impact. This study highlights that, as different processes govern NO_3^- pollution and Cl^- salinization, an informed management is essential to effectively tackle protection measures to safeguard groundwater resources. The protocol here employed can be extended to other regions, assisting policymakers and managers in identifying areas exposed to potential human and naturally driven pollution processes.

Keywords Gaussian imulation · Probability mapping · Machine learning · Nitrate pollution · Chloride salinization · Groundwater resources

Extended author information available on the last page of the article

Published online: 25 April 2025

1 Introduction

The declining quality of freshwater resources, stemming from both natural and anthropogenic processes, has become one of the most alarming and widespread issues in the Mediterranean Region. This is particularly concerning when considering groundwater reserves, which constitute the largest source of freshwater supply worldwide (Gleeson et al. 2020; Balacco et al. 2023). The use of groundwater resources, potentially polluted, for drinking or irrigation purposes can be hazardous to humans and plants' health. The phenomenon of groundwater pollution can take various forms, and NO_3^- stands out as a prominent pollutant (Ascott et al. 2017). The source of NO_3^- into groundwater is often linked to human activities, such as agriculture or municipal wastes (Stevenazzi et al. 2017), that may release other pollutants in groundwater, thus complex relationships can be found with others chemical species according to the pollution sources (Busico et al. 2018; Mastrocicco et al. 2021). Furthermore, the salinization of groundwater, mainly related to Cl^-, is on the rise in several coastal plains, primarily because of climate variability and groundwater overexploitation (Boufekane et al. 2022; Ez-Zaouy et al. 2023). Several processes can be responsible to trigger and increase the risk of groundwater pollution/salinization, such as: (i) leaks from industrial or residential wastewater systems, (ii) agriculture leaching, (iii) water-rock interaction, and (iv) actual/paleo seawater intrusion. This complexity can deeply exacerbate the challenges associated with groundwater quality assessment and monitoring (Bordbar et al. 2023a; Ouarani et al. 2023; Li et al. 2023). In recent years, the assessment of risks related to groundwater salinization and pollution has garnered the attention of scientists. This assessment examines three key aspects: (i) groundwater vulnerability which assesses the intrinsic susceptibility of a specific aquifer to salinization and pollution processes (Machiwal et al. 2018); (ii) the source of the risk which aims at identifying the processes responsible for the pollution/salinization status (Mastrocicco et al. 2021); and (iii) the potential damage from salinization/pollution (Xu et al. 2023) which reflects the prospective usage of groundwater (Bordbar et al. 2023a). Various methods have been proposed to assess and map the probability of groundwater pollution and salinization, including rating indices, statistical techniques, numerical and hybrid models (Adhikary et al. 2011; Li et al. 2015; Zeng et al. 2016; Islam et al. 2017; Bodrud-Doza et al. 2019; Busico et al. 2020; Wang et al. 2023). Although these methods provide insightful information, they frequently involve methodological subjectivity, computational difficulties, large data inputs, availability of water quality and suffer data smoothing effect (Chica-Olmo et al. 2014; Busico et al. 2018; Khosravi et al. 2021; Bouhout et al. 2022; Taghavi et al. 2022; Rama et al. 2022; Khan et al. 2023; Luo et al. 2023). A rising methodology in environmental studies is the deployment of stochastic simulations, a computational technique used to model and analyze systems that involve random or probabilistic elements. Stochastic simulations try to reproduce the main statistical measures of dataset distribution, including histogram and spatial continuity, calculating a set of alternative random images allowing uncertainty analysis (Cinnirella et al. 2005). Sequential Gaussian Simulation (SGS) is a widely used simulation method in many fields related to geoscience, such as soil and water science (Lv and Wang 2019; Bai and Tahmasebi 2022; Akbulut Özen et al. 2022; Karami et al. 2022; Busico et al. 2024). SGS algorithm is, by assumption, a multi-Gaussian random function model (Aryafar et al. 2020) that can keep the spatial structure of variables to produce results of an unknown spatial distribution, partially reducing the smoothing effect of kriging (Ma et al. 2022).

To make the assessment even harder, several socio-economic parameters could influence groundwater pollution and salinization. Among the socio-economic factors, deforestation, urban planning, industrial effluent discharge, domestic and commercial sewage deposition, agriculture, aquaculture, and mining are directly or indirectly responsible for groundwater contamination. While information related to the main hydrogeological parameters (i.e., water depth, lithology, recharge, and soil properties) is nowadays made available in "Open databases" with satisfactory resolution and data consistency (Abbaspour et al. 2019; Rama et al. 2022), information regarding anthropogenic and socio-economic pressures is still lacking, especially considering regulated and unregulated nutrient discharge. Consequently, this kind of data suffer from high uncertainty and are deeply dependent on researcher's assumptions (Malagó and Bouraoui 2021). The importance of these parameters in each basin depends on its intrinsic hydrogeological features and on the investigated processes (Bordbar et al. 2023b). By identifying the most important factors, management plans can be designed to achieve sustainable management of freshwater resources and avoid groundwater quality deterioration. So far, different feature selection methods have been used in various studies to assess the prioritization of parameters affecting groundwater pollution and salinization. Among these, machine learning methods such as Decision Tree (DT), Random Forest (RF), and Information Gain Ratio (IGR) have been used in studies related to groundwater vulnerability (Sun and Hu 2017; Khosravi et al. 2018; Chowdhuri et al. 2021; Bordbar et al. 2022; Pourghasemi et al. 2023), and groundwater quality assessment (Bordbar et al. 2023a). Anyway, the intrinsic structure of each algorithm could generate different results retaining the same input dataset, making mandatory an in deep discussion of the obtained results. In particular, the evaluation of the physical plausibility of the behavior of the modelled parameters is essential for the validity of the assessment (e.g., Bajni et al. 2023; Bordbar et al. 2023b). Nonetheless, only a few studies attempt a comparison of different machine learning methods with a consistent discussion of the results obtained from an environmental point of view.

Considering this scenario, the main objectives of this study are: (i) to produce probability maps for NO_3^- pollution and Cl^- salinization using SGS, (ii) to compare probability maps with the regional groundwater quality monitoring network and (iii) to assess the relative importance of several hydrogeological and socio-economic parameters in determining the spatial probability of NO_3^- pollution and Cl^- salinization. The areas of interests are three alluvial plains located within the Campania Region in southern Italy.

1.1 Study areas

Three different areas within the main alluvial plains in the Campania Region (southern Italy) were considered for this study (Fig. 1): (i) the low Volturno plain (LVP), (ii) the Garigliano plain (GP), and the high Volturno plain (HVP). LVP is a large graben filled with a succession of marine, coastal, alluvial, and volcanic deposits, where the main outcropping lithologies are volcanic and alluvial materials. The alluvial deposits comprise a heterogeneous mixture of sand, silt, and clay, which have been deposited by the Volturno River. The volcanic materials are made of tuffs and other volcanic products (i.e., pyroclastic deposits mainly from fallout) generated through multiple explosive events associated with the Phlegrean Fields volcanic complex. Among these events, the Campanian Ignimbrite eruption (~39 ky Before Present) caused the deposition of greyish cinerites (i.e., tuffs) associated with black

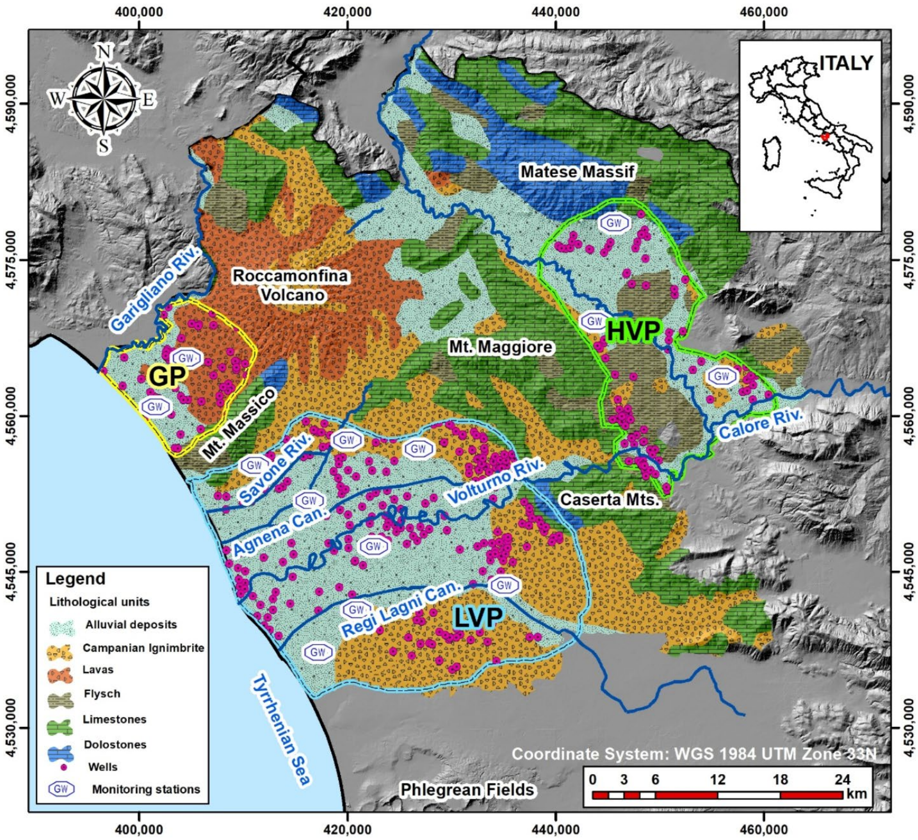

Fig. 1 Study areas with the main outcropping lithologies and the wells' locations (LVP: low Volturno plain, GP: Garigliano plain, and HVP: high Volturno plain)

scoriae and lava shreds, either in lithoid, incoherent, or scoriaceous facies, outcropping close to the reliefs (De Vita et al. 2018). GP is a smaller graben than LVP, also characterized by the deposition of coastal, alluvial, and volcanic materials. It hosts sedimentary deposits from the Miocene to Quaternary periods, as well as continental clastic sediments originating from the Garigliano River. GP also features volcanic debris deposits originating from the Roccamonfina volcano (Ducci and Sellerino 2013). In HVP the outcropping lithological units include: (i) limestone at the foothills of Mt. Maggiore and Caserta Mts., (ii) volcanic deposits in the northern segment of the study area, (iii) alluvial sediments originating from the Volturno River, and (iv) an arenaceous-clayey flysch made of mixed conglomerates, sandstones, marls, and clays, which outcrop in the middle of the plain. The climate in the three areas is Mediterranean with hot and dry summers and wet winters in the coastal areas, moderate and humid in the inland areas. A large temperature difference is recorded between the mountain ranges and the alluvial plains (Rufino et al. 2019). Intense human activities take place in the three plains, causing an impact on the land cover/use. In these plains, agricultural fields cover more than 65% of the land while residential areas range between 10 and 25%. A small portion of the territory is covered by woods and forests, especially along the shoreline of GP and LVP and on the relief of HVP. The two coastal plains, GP and LVP, are connected and widely affected by agricultural and urban areas, here big farms and zootechnic activities coexist with small agricultural fields within the sub-urban areas, while densely populated cities are located near mountain ranges and along the coastline. In HVP, where agricultural activities are dominant, urban areas are restricted to the gentle carbonate slopes surrounding the plain. The aquifer under investigation is represented by the shallow unconfined aquifer mainly hosted within alluvial (loamy textured) and reworked volcanic material in both GP and LVP while within HVP the saturated zone is mainly made of coarse alluvial/colluvial materials. The groundwater head range from −3 m to 25 m b.s.l. in LVP and GP while range from 50 to 75 m b.s.l. in the HVP (Allocca et al. 2007) (Fig. S1). Detailed information about the geographical, climatic, geological, hydrogeological and land cover/land use characteristics of the study areas are summarized in the Supplementary Material (S1.1-3) and fully reported in Busico et al. (2018); Mastrocicco et al. (2021); Bordbar et al. (2023a), and the references therein.

1.2 Modeling framework

The study is structured following three main steps (Fig. 2). First, the probability maps of NO_3^- pollution and Cl^- salinization were created for the three areas, using SGS. Two thresholds' values were set for NO_3^- (40 mg/L for potability use) and for Cl^- (90 mg/L for irrigation). For NO_3^-, the water quality standard from WHO was considered (WHO 2017), while for Cl^- the suggested concentration for sensible crops from FAO Irrigation Water Quality Guidelines has been used (Misstear et al. 2006). The decision to stay slightly below the two limits (50 mg/L for NO_3^- and 100 mg/L for Cl^-) was made for precautionary reasons allowing an optimal spatial distribution of those areas close to the warning concentrations. Second, the values of probability, coming from SGS, were used to determine the priority of factors potentially affecting pollution and salinization for each study area. Specifically, three fishnets with a 100 × 100 m spatial resolution were created to sample the raster probability value obtained by the previous SGS application, and to create an input dataset for machine learning algorithms. DT, RF, and IGR were used to determine the priority of factors affecting pollution and salinization. For DT modeling, actual measurements of Cl^- and NO_3^- probability (%) were used. In contrast, IGR and RF categorized the data into two groups: one labeled as 0 (below the median of the obtained probability) and the other as 1 (above the median of the obtained probability). Since each method can provide different results, a rank from 1 (least important) to 6 (most important) was assigned for each NO_3^- polluting factor and a rank from 1 (least important) to 7 (most important) was assigned for factors affecting Cl^- salinization. Then, a summary was made by summing up the ranks obtained through the application of the three machine learning algorithms to assess the impact of each parameter on pollution/salinization.

The three study areas were selected for their distinct hydrogeological and socio-economic characteristics. LVP and GP are both alluvial plains; however, they significantly differ in geological composition (i.e., LVP consists of tuff and alluvial deposits, whereas GP is dominated by lava formations). Additionally, their morphological conditions vary, with LVP experiencing a high subsidence rate compared to GP (Matano et al. 2018). Despite both being primarily agricultural areas, LVP also features a complex suburban network, introducing additional anthropogenic impacts. When comparing LVP and HVP, although

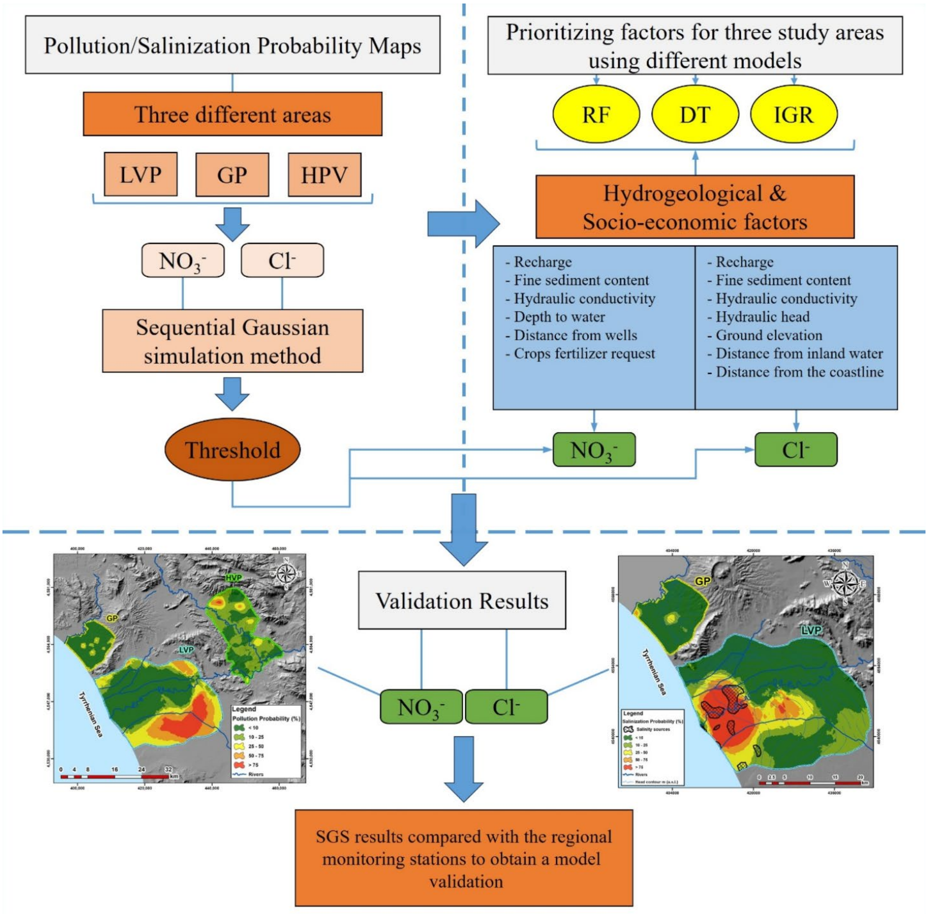

Fig. 2 Flowchart applied in the study areas (LVP: low Volturno plain, GP: Garigliano plain, HVP: high Volturno plain, RF: Random Forest, DT: Decision Tree, and IGR: Information Gain Ratio)

both belong to the Volturno basin, they exhibit notable differences in geology, primary recharge sources, and socio-economic activities. For more info regarding study area characteristics refer to Supplementary Material (S1.1-3). These variations across the three study areas enable a comprehensive evaluation of each factor's role while also highlighting how the same factor may influence different environments in distinct ways and to obtain more reliable results of likelihood of groundwater pollution and/or salinization. Nitrate pollution was investigated in all three study areas, whereas Cl^- salinization was further investigated only in the coastal study areas (i.e., LVP and GP) since the HVP exhibits a likelihood of Cl^- higher than 0% (always below 90 mg/L).

Seven and six factors were selected as potentially affecting groundwater pollution and salinization, respectively (Fig. 2). These factors have been considered as the input of each algorithm, and the result of probability maps has been used as dependent variable to achieve the final ranking output. As a rule, the main hydrogeological (e.g., hydraulic head, recharge, distance from inland water, distance from the coastline, ground elevation, hydraulic conductivity, fine sediment content, and depth to water table) and socio-economic parameters (e.g., crops fertilizer request and distance from wells), commonly used in groundwater vulnerability assessment and available in open repositories, were tested in this work (Machiwal et al. 2018; Bordbar et al. 2023a). The choice of using mainly open data will allow modelling replicability since most of the data used has smooth resolution and worldwide extension. Hydrogeological factors were considered for their impact on transport and dilution of pollutants and/or salt, while socio-economic factors were chosen as proxies for anthropogenic impacts and landscape modification. Regarding the socio-economic parameters, the load of nutrients for each crop has been used as “crops fertilizer request”. The values of fertilizers and manure have been sourced from Ministero delle Politiche Agricole, Alimentari e Forestali (MIPAF) guidelines for the Campania Region. Similarly, the distance from wells and artificial canals were considered as a degree of anthropogenic pressure. Sources, resolution, explanation and spatial distribution of the selected parameters are available in the Supplementary Material of Bordbar et al. (2023a) and freely downloadable from the website: https://www.datasetw4all.info/.

Lastly, the third step represents the validation phase, obtained by comparing the probability maps obtained with SGS (i.e., probability of exceeding the threshold value) with the probability of exceeding the same threshold limits of NO_3^- and Cl^- measured at 13 monitoring wells belonging to the regional groundwater quality monitoring network of the Campania region located within the three study areas (Fig. 1) and offering a long term monitoring (Agenzia Regionale Protezione Ambiente della Campania - ARPAC, https://dati.arpacampania.it/group/acque-sotterranee).

A different source of water quality data has been preferred instead of using a split percentage of the internal database, since the water quality network provides a temporal evaluation of the data (2–3 data per year, for almost 10 years) which allows a more robust validation of the probability of pollution and salinization, partially overcoming the issue of data staticity.

Details about the applied methods and the datasets used in this study are reported in the Supplementary Materials (S1.4-6).

2 Results

2.1 SGS results for probability maps

The probability maps for NO_3^- and Cl^-, obtained using the WHO and FAO drinking water standards as cutoff values, are represented in Figs. 3 and 4. The maps were categorized into five probability classes: very low (0–10%), low (10–25%), medium (25–50%), high (50–75%), and very high (75–100%). Concerning the result for LVP (Fig. 3), the NO_3^- probability ranges from 0 to 97%, with a very low probability in the middle of the plain, where the alluvial deposits laid by the Volturno River outcrop. The highest probability of exceeding 40 mg/L corresponds to the volcanic deposits in the south, east, and northern sectors, at the foot of the mountain reliefs. The Cl^- salinization probability (Fig. 4) ranges from 0 to 100% showing the highest probability in the western area, up to 15–20 km from the coastline, with a tendency of decrease moving away from the coastline towards the carbonate reliefs, somewhere interrupted by small high probability spots. In GP the highest probability of NO_3^- pollution and Cl^- salinization is 60% and 77%, respectively (Figs. 3 and 4). The high-

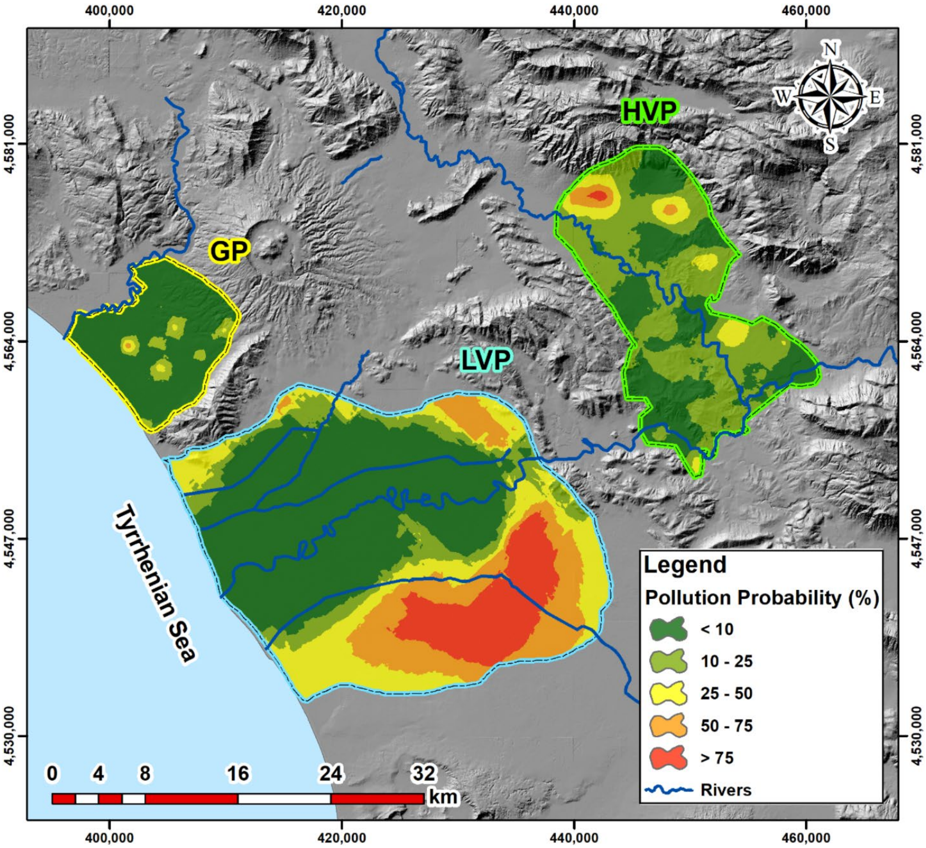

Fig. 3 Pollution probability (%) for NO_3^- (possibility to be higher than 40 mg/L) for LVP, GP, and HVP

est probability of exceeding NO_3^- threshold is in specific spots in the middle of the plain, whereas the highest probability of exceeding Cl^- is near the Garigliano River mouth and in a small area in the center of the plain. For HVP only the NO_3^- probability map is presented, as the selected cutoff value for Cl^- (90 mg/L) is never observed in this area. The NO_3^- probability (Fig. 3) ranges from 0 to 84%: high probability values are in the northern sector, on the left bank of the Volturno River, whereas low probability values are in the eastern and southern sectors, along the Calore and Volturno Rivers.

2.2 Prioritizing the parameters affecting NO_3^- pollution and Cl^- salinization

The prioritization of parameters influencing NO_3^- pollution and Cl^- salinization in LVP, GP, and HVP was carried out using DT, RF, and IGR (Fig. 5). Notable differences in the ranking of parameters can be observed. For LVP, a general agreement among DT and IGR regarding the low importance of “crops fertilizer request” and “distance from wells” is evident, while both IGR and RF highly prioritize “depth to water”. The three algorithms rank “fine sediment content” in an identical way, and DT and RF align on the high importance of the “recharge” parameter. For the parameters affecting Cl^- salinization only two matches are

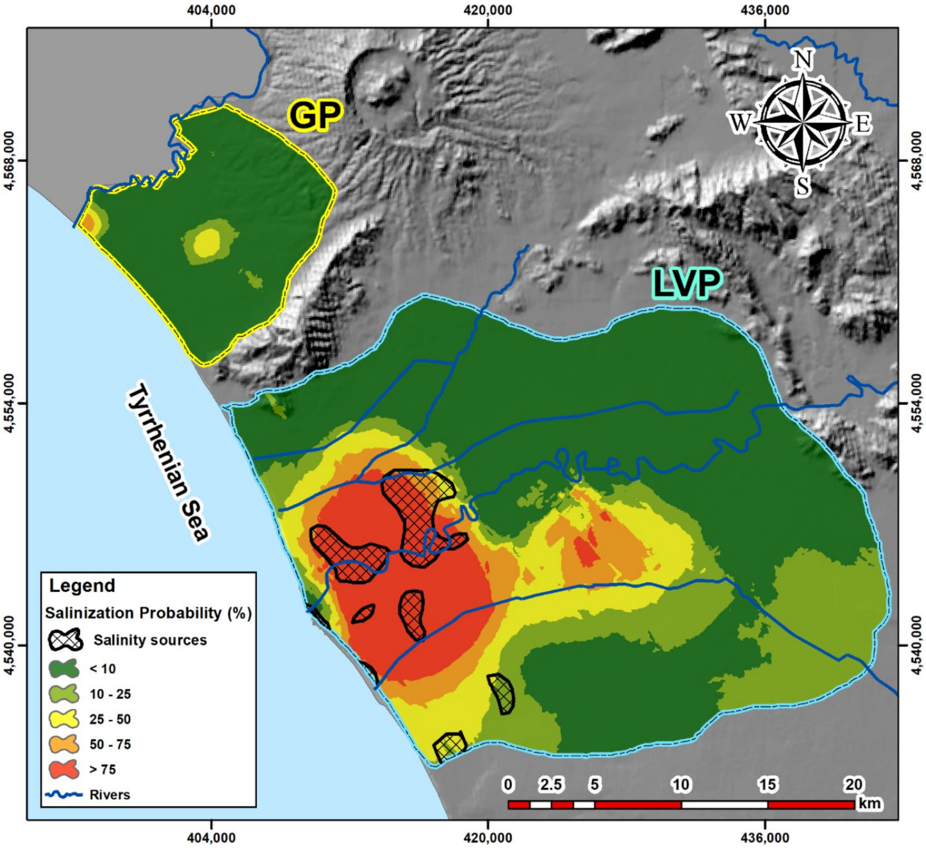

Fig. 4 Salinization probability (%) for Cl- (possibility to be higher than 90 mg/L) for LVP and GP. Salinity sources from Schiavo et al. (2023)

evident: IGR and RF for "fine sediment content", and DT with RF for "distance from inland water". An agreement among the three algorithms in the ranking of the seven parameters has never been found. Similar results were observed in GP and HVP areas, with some agreements in classification, though there are more marked differences in Cl^- ranking compared to NO_3^-. Differences in parameter ranking among the three study areas were expected due to their significantly varying hydrogeological conditions. Regarding NO_3^- in GP, DT and RF agree in highly prioritizing "hydraulic conductivity" and "depth to water". Similarly, the two algorithms also agree in recognizing the low importance of "distance from wells" and "crops fertilizer request". All algorithms agree in ranking "fine sediment content" and "recharge". Considering Cl^- salinization, both DT and RF highly prioritize "distance from inland water", while IGR and DT agree on the "ground elevation" ranking. As for the LVP study area, an agreement among the three algorithms in the ranking of the seven parameters has never been found. Finally, for HVP, only two matches are evident among DT and IGR for "hydraulic conductivity" (high rank) and among DT and RF for "fine sediment content" (low rank). However, the observed discrepancies within the same study area can be attributed entirely to the structure of the used algorithms, since also the number of input data

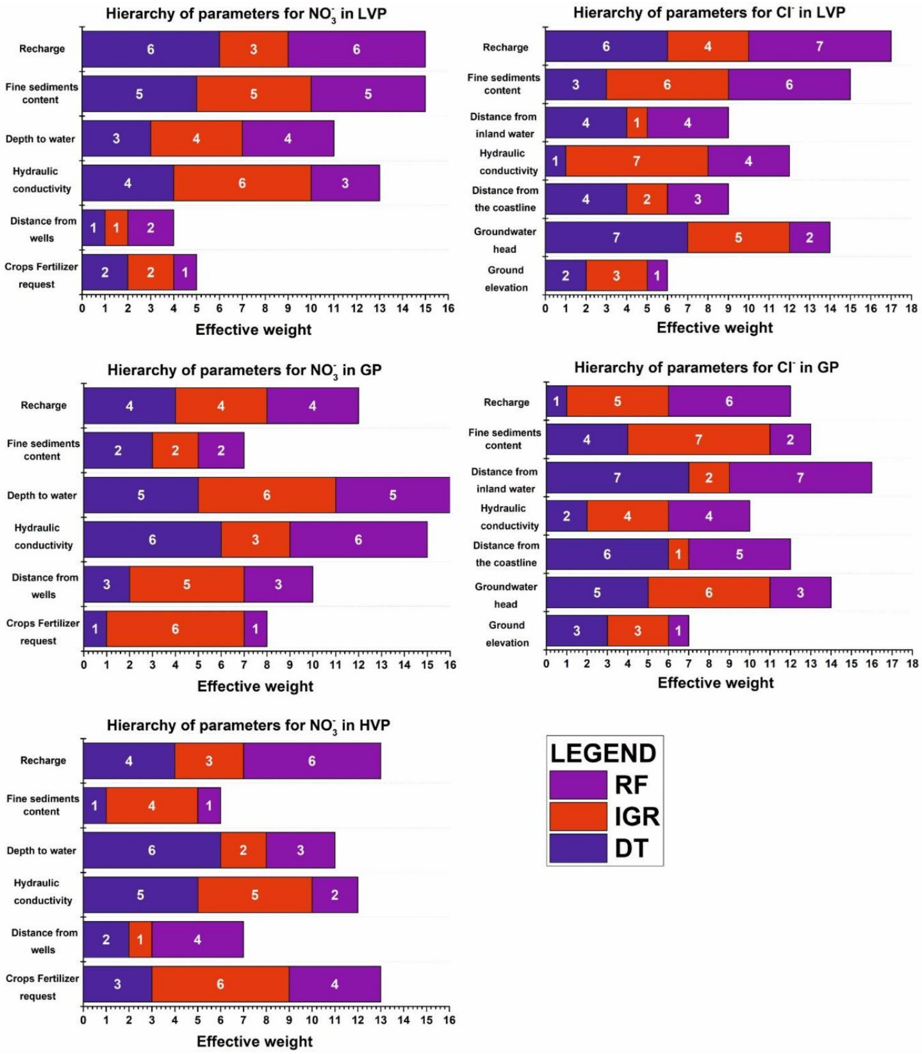

Fig. 5 Hierarchy of parameters for the three study areas (RF: Random Forest, DT: Decision Tree, and IGR: Information Gain Ratio)

remains the same for each algorithm in the different study areas (251 for LVP, 54 for GP, and 118 for HVP). Another explanation could be related to the data input for each algorithm. In fact, while IGR and RF used 0–1 values based on the separation rule previously described, DT used untransformed values. Nonetheless, significant differences are still evident between IGR and RF, underscoring the need for a thorough understanding and discussion of the hydrogeological characteristics of the study area to determine the most appropriate results. As previously stated, the DT model used actual values of NO_3^- and Cl^-, while the RF and IGR models categorized the data into binary classes (0 and 1). This difference in data handling was intended to explore how model outputs would vary when continuous values (DT model) were used instead of binary classification (RF and IGR models). The comparison

Table 1 Summary of prioritizing parameters affecting NO_3^- pollution

LVP	Rank Sum	GP	Rank Sum	HVP	Rank Sum
Recharge	15	Hydraulic conductivity	16	Recharge	13
Fine sediment content	15	Depth to water	16	Crops fertilizer request	13
Hydraulic conductivity	13	Recharge	13	Hydraulic conductivity	12
Depth to water	11	Fine sediment content	8	Depth to water	11
Crops fertilizer request	5	Distance from wells	7	Distance from wells	8
Distance from wells	4	Crops fertilizer request	3	Fine sediment content	6

Table 2 Summary of prioritizing parameters affecting Cl^- salinization

LVP	Rank Sum	GP	Rank Sum
Recharge	17	Distance from inland water	16
Fine sediment content	15	Hydraulic heads	14
Hydraulic heads	14	Fine sediment content	13
Hydraulic conductivity	12	Distance from the coastline	12
Distance from inland water	11	Recharge	12
Distance from the coastline	9	Hydraulic conductivity	10
Ground elevation	6	Ground elevation	7

of model performances and outcomes across these approaches provided insights into how each model responded to data conversion from continuous variables to categorical classes.

To ensure a balanced evaluation, the final ranking was derived by summing the ranks from all three models, preventing any single model's limitations from disproportionately influencing the results. However, these methodological differences introduce some degree of uncertainty in factor ranking, emphasizing the need for hydrogeological reasoning when interpreting the results. Additionally, variations in model outputs suggest that certain parameters may hold high significance in specific conditions but may be less relevant in a broader context, requiring careful contextual analysis.

2.3 Sum of the prioritization of models

The results of factor prioritization show, as expected, that the effect of each parameter on both NO_3^- pollution and Cl^- salinization greatly varies using different models in the same area and among the three areas. Therefore, a summary was made for each chosen factor based on the considered rankings. The results of this summary (Table 1) show that the most important factor controlling NO_3^- pollution in LVP is recharge, followed by fine sediment content, hydraulic conductivity, and depth to water. The socio-economic parameters indicating human pressure (namely crops fertilizer request and distance from wells) have instead the lowest impact. The results are different in GP, where hydraulic conductivity and depth to water show the highest impact on NO_3^- pollution, followed by recharge and fine sediment content. Instead, like in LVP, distance from wells and crops fertilizer request occupies the last ranking position. The most influential parameters on NO_3^- pollution in HVP are recharge and crops fertilizer request, followed by hydraulic conductivity, depth to water, distance from wells, and fine sediment content. The parameters affecting Cl^- salinization (Table 2) in LVP, from the most to the least influencing one, are: recharge, fine sediment

Table 3 Correlation between parameters for NO_3^- pollution and Cl^- salinization

Parameter	Correlation with NO_3^- for LVP	Correlation with NO_3^- for GP	Correlation with NO_3^- for HVP	Parameter	Correlation with Cl^- for LVP	Correlation with Cl^- for GP
Recharge	-0.36	-0.11	-0.4	Recharge	-0.2	-0.16
Fine sediment content	-0.49	-0.06	0.2	Fine sediment content	0.33	0.04
Hydraulic conductivity	0.01	-0.06	-0.26	Hydraulic heads	-0.51	-0.06
Depth to water	-0.07	0.08	0.09	Hydraulic conductivity	0.07	-0.07
Crops fertilizer request	-0.26	-0.01	0.64	Distance from inland water	-0.56	-0.05
Distance from wells	0.22	-0.08	-0.48	Distance from the coastline	-0.56	-0.08
-	-	- -		Ground elevation	-0.41	-0.06

content, hydraulic heads, hydraulic conductivity, distance from inland water, distance from the coastline, and ground elevation. Whereas, from the most to the least influencing factor on Cl^- salinization in GP there are: distance from inland water, hydraulic heads, fine sediment content, distance from the coastline, recharge, hydraulic conductivity, and ground elevation.

3 Discussion

3.1 Correlation evaluation

A positive or negative correlation between the investigated parameters for NO_3^- pollution and Cl^- salinization has been defined to explain the results in detail (Table 3). Similarly to multivariate statistical analysis such as Factor Analysis and Principal Component Analysis, the output of DT algorithm allows us to discuss the positive or negative correlation among the chosen parameters and the dependent variable (NO_3^-, Cl^-), along with their magnitude of correlation. Considering the possibility of NO_3^- pollution, recharge plays a primary role in all the study areas, influencing dilution processes. However, the primary factor leading to low NO_3^- probability in the LVP (green areas) is attributed to the presence of soil organic matter (SOM) in clay and peaty lenses (Busico et al. 2018), as testified by the magnitude and negative correlation with the fine sediment content parameter. The rapid water flow within this region also plays a significant role in regulating NO_3^- pollution since the presence of tuff (i.e., lithoid or scoriaceous facies) has led to an increase in groundwater flow velocity, raising the risk of NO_3^- pollution and the transport of pollutants from one point to another. Despite the intensive agricultural activity, all the main crops are low fertilizer demanding (i.e., vegetables, barley, or wheat), which contributes to lowering the weight of agricultural pressure compared to the other parameters. Similarly, in GP the agricultural pressure parameter occupies the lowest rank with negative correlation. This phenomenon can be attributed to the types of crops cultivated in these areas, which necessitate a low amount of chemical fertilizers, like in LVP, and to peculiar soil characteristics (namely the high SOM content), which favors natural attenuation processes. In both LVP and GP, sewage emerges as the predominant source of NO_3^- pollution, resulting in agricultural pressure ranking lowest in significance (Busico et al. 2018, 2020). In HVP, the high positive correlation with agricultural pressure and the high negative correlation with the distance from wells testify the influence of anthropogenic pressure in determining groundwater quality and thus in defining the likelihood of NO_3^- pollution. Local environmental conditions do not promote NO_3^- degradation since the soil is coarsely textured with a low amount of SOM due to its colluvial nature.

The salinity in LVP results from paleo seawater entrapped in the fine lenses deposited during the late Holocene transgression (Schiavo et al. 2023). In LVP, recharge emerges as the key parameter, exerting significant influence on Cl^- salinization, displaying a negative correlation. This indicates that the likelihood of groundwater salinization increases with reduced recharge, as the dilution processes facilitated by incoming freshwater diminish, thereby accentuating salt accumulation. A positive correlation, due to the spatial coexistence of high Cl^- probability with the amount of fine sediment was observed, indicating that Cl^- concentration increases in correspondence of those areas with a high silt and clay content. The negative correlation with the hydraulic heads indicates that when the groundwater level is below sea level the possibility of salinization increases due to both actual seawater intrusion (SWI) and seepage of paleo seawater. However, the third-ranking influence of this parameter, coupled with the low weight assigned to the distance from the coastline (Table 2), suggests that an extended actual SWI is unlikely to occur in this area. A negative correlation is also evident with ground elevation since most of the areas affected by high Cl^- probability are below the sea level. In GP, there is a negative correlation between the distance from the superficial body and Cl^- values. This indicates that salinization increases by reducing the distance from the superficial body and conversely, thus SWI in GP is directly influenced by the Garigliano River (Fig. 4). A negative correlation was found for the hydraulic head, as in LVP.

3.2 Probability of NO_3^- pollution and Cl^- salinization

By comparing the three areas, the highest probability of both polluted and high saline water occurs in LVP, whereas the probability of pollution in HVP is higher than in GP. It is worth mentioning that HVP is not affected by groundwater salinization. To validate the results, probability estimates were compared with chemical data from the regional groundwater monitoring network. Specifically, 13 and 10 monitoring wells measuring for NO_3^- and Cl^- concentrations, respectively were used. The probability of exceeding 40 mg/L of NO_3^- and 90 mg/L of Cl^- was calculated for each monitoring well using semi-annual time series spanning 10 years. These probability values were then compared with those obtained through SGS in the same "pixel" point location. To ensure consistency in the comparison, the "Raster to Point" tool was used to extract SGS values at the exact locations of the monitoring wells, enabling a direct cross-analysis of the data.

The results show a coefficient of correlation (R^2) of 0.97 for NO_3^- and 0.67 for Cl^-, making the SGS results highly reliable especially for NO_3^- pollution (Fig. S2). The spatial distribution of NO_3^- probability in LVP strictly follows the deposits' distribution. The lower probability is connected to the alluvial deposits near the Volturno River, where, despite the agricultural vocation of the area, the high percentage of fine sediments along with the highly reducing conditions represent a natural barrier against NO_3^- pollution (Ducci et al. 2016; Busico et al. 2018). NO_3^- levels in LVP remain low due to the presence of peaty layers, containing a significant amount of SOM, which creates reducing conditions capable of degrading NO_3^- (Mastrocicco et al. 2013). To confirm this assumption, the average SOM content in the soil across different areas within the plain, divided based on geological features into alluvial and volcanic regions, was investigated and reported in Table S1. Data were elaborated from SIAS project (Sviluppo di Indicatori Ambientali sul Suolo in Italia - Development of Soil Indicators in Italy) and ISCRIC database (Batjes et al. 2017; Poggio et al. 2021). In LVP, alluvial deposits, hosting the major portion of the agricultural area, exhibit SOM levels approximately ten times higher than those found in volcanic deposits, which in turn host most of the urban areas of the plain. Consequently, in agricultural areas SOM acts as a buffering against NO_3^- pollution, whereas urban areas are not warded by this buffer capacity and moreover host a dense municipal wastewater system, leading to a high probability of sewer leaching. The areas with the highest probability of pollution overlap with fractured tuff deposits. These post-depositional fractures, decrease the residence time in the unsaturated zone and create preferential pathway for pollutants migration. Additionally, the proximity of urban areas highlights the significant contribution of sewer leakage and suburban agricultural activities to groundwater pollution (Rufino et al. 2019). Within HVP, consisting solely of coarse-sand textured alluvial deposit, derived by the surrounding calcareous and terrigenous rock formations, SOM is low (around 7.66%) compared to both LVP and GP, offering a lower buffer against NO_3^- pollution compared to LVP. Conversely, in GP the percentage of SOM is notably higher than in alluvial areas due to the presence of highly porous lava deposits, which could foster the development of SOM (Candra et al. 2023). Accordingly, the probability of NO_3^- pollution is low in GP, with only a few identified hotspots, primarily within urban centers. Regarding Cl^- salinization, the higher probability in LVP insists in a large area in the western sector, near the coastline up to 15 km inland. The more pronounced impact of salinization is concentrated in the coastal region, where the proximity of shallow marine sediments near the mouth of the Volturno River and the ongoing SWI lead to elevated levels of electrical conductivity, Na^+, and Cl^- in groundwater. The analysis of salinization probability reveals that the contribution of actual SWI close to the coastline is negligible. This finding is supported by previous studies on the same area using Monte Carlo Simulation (Schiavo et al. 2023), multivariate statistical analysis (Busico et al. 2018), rating index (Busico et al. 2021), and numerical simulations (Gaiolini et al. 2023), which also located the main source of Cl^- inland (Fig. 4), as per our probability distribution. In this area, paleo seawater entrapped in Holocene fine lenses significantly increases Cl^- levels, exceeding the used threshold. Some hotspots in the center of the plain are due to sewer leaching and/or zootechnic activity which could increase both NO_3^- and Cl^- concentrations in groundwater.

Considering the prioritizing factors for the probability of NO_3^- pollution, the crucial role of recharge, fine sediment content, hydraulic conductivity, and depth to water table is consistent with the hydrogeological conditions, since pollutants' movement, dilution, and degradation are all connected to those parameters. For Cl^- instead, the lower importance of the distance to the coastline further strengthens the role of paleo seawater which spatially overlaps areas where a high percentage of fine sediments occur.

In HVP the probability of NO_3^- pollution is higher in agricultural areas where crops requiring high fertilization are harvested (e.g., corn, vegetables, and fruit trees), making water quality unsuitable for potable use (Rufino et al. 2019; Bordbar et al. 2023a). In this area the presence of coarse colluvial deposits of carbonate origin does not offer the same degradation barrier against NO_3^- pollution as in LVP. This is confirmed by the prioritization results where higher and lower impacts are assigned to crops fertilizer request and fine sediment content, respectively.

GP is less affected by both NO_3^- pollution and Cl^- salinization probability with a maximum probability of 60% and 77%, respectively. The higher probability of NO_3^- pollution appears in the central area of the plain characterized by volcanic deposits and high agricultural impact, which make the area more vulnerable (Busico et al. 2021). Moreover, the fractured nature of lava deposits allows the faster movement of polluted water as confirmed by the high impact of hydraulic conductivity. Regarding Cl^- salinization, the higher probability is detected near the Garigliano River mouth, as reported in a previous study where negative base exchange index (BEX) and alarming values of sodium adsorption ratio (SAR) have been calculated (Mastrocicco et al. 2021). Accordingly, the distance from superficial bodies and the coastline, and the hydraulic heads show the highest impact in determining the probability of salinization.

Summarizing, the factors affecting NO_3^- pollution and Cl^- salinization varies in importance in the three areas. Based on the obtained results, it was found that morphology and the distance from inland water and the coastline become more prominent in LVP than in GP, since the processes that influence Cl^- salinization are different. However, the role of recharge, fine sediment content, and hydraulic conductivity are slightly lower in LVP compared to GP (Table 2). Hydraulic heads are equally important in LVP and GP. Considering NO_3^- pollution, the importance of recharge, fine sediment content, and hydraulic conductivity is higher in LVP than in HVP. Crops fertilizer request and distance from wells are less important in LVP than in HVP, while depth to water has a constant role in both LVP and HVP. The parameters of recharge, fine sediment content, and crops fertilizer request are more important in LVP than in GP. Whereas hydraulic conductivity, depth to water, and distance from wells are less important in LVP than in GP.

3.3 Advantages and drawbacks of the implemented models

SGS is commonly utilized by professionals owing to its straightforward theoretical concepts, easy numerical implementation, and adaptability, though its primary drawback is the high computational demand (Nussbaumer et al. 2018). The main issue with SGS is its computational efficiency, especially when dealing with large datasets comprising hundreds of thousands of points. This challenge arises from the need to solve a substantial linear system of equations in each iteration, involving both newly sampled and previously simulated points for building the covariance matrix. If N points are involved, the computational complexity to obtain the solution is approximately $O(N^3)$ (Bai and Tahmasebi 2022). In addition, this study used different algorithms to prioritize parameters for NO_3^- pollution and Cl^- salinization. Each implemented algorithm has its advantages, and the choice of the feature selection technique depends on the dataset, the problem at hand, and the computational constraints. It is often beneficial to experiment with multiple techniques to identify the one that works best for a specific task. The total weights obtained for each parameter can provide a general estimate of the impact of the parameter. As mentioned earlier, the actual values of Cl^- and NO_3^- were utilized for DT modeling, while for running RF and IGR the data were categorized into two classes of 0 and 1. In this study, it has been avoided employing feature selection methods to mitigate subjective judgment and, instead, the ranking of the features was preferred to show their relative importance. These models can be applied in the preliminary phases of a study to evaluate the predictive potential of factors. Assessing the importance of these factors before the modeling stage enables the identification and exclusion of parameters with minimal impact in some scenarios. Another important limitation is the availability of socio-economic parameters, which have a significant impact on groundwater pollution and salinization. While most studies focus on groundwater vulnerability to physical or hydrogeological factors, socio-economic aspects have received less attention. One key reason is that hydrogeological parameters are often accessible in open databases, whereas socio-economic data is more challenging to obtain. Information such as sewer and septic tank locations or other diffuse and point pollution sources is often difficult to spatially discretize within a study area. Further elaboration could integrate the distance from urban areas or from specific highly impacted agricultural activities as surrogate to account for other possible pollution sources.

Summarizing, the implemented methods have greatly improved the understanding of the processes of salinization and groundwater pollution in the studied area. Furthermore, prioritizing hydrogeological and socioeconomic criteria allows for a more effective assessment of pollution and salinization factors, paving the way for targeted and evidence-based groundwater management strategies. This understanding is crucial for policymakers and stakeholders to implement effective mitigation strategies in high vulnerability areas.

4 Conclusions

This research was conducted with the aim of assessing the probability of NO_3^- pollution and Cl^- salinization to assist policymakers and managers in pinpointing regions susceptible to groundwater degradation. The following steps were undertaken for this assessment:

1. Realization of the probability maps: a geostatistical simulation method based on SGS was used to reconstruct the spatial distribution of NO_3^- pollution and Cl^- salinization.
2. Evaluation of the importance of variables affecting pollution/salinization: three different techniques (DT, RF, and IGR) were used to assess the relative importance of each parameter by considering the threshold for Cl^- salinization and NO_3^- pollution. Summaries were generated for each parameter by considering the resulting ranks.
3. Validation of the probability maps: the possibility of exceeding 40 mg/L for NO_3^- and 90 mg/L for Cl^- was computed by analyzing monthly time series spanning over 10 years. The resulting probabilities were compared with values derived from the SGS implementation.

The results obtained in this study were as follows:

1. Regarding the probability of NO_3^- pollution in LVP, there is a notably low likelihood in the central plain, thanks to the alluvial deposits rich in SOM. Considering the Cl^- salinization probability, the highest likelihood is observed in the western area of LVP, extending up to 15–20 km inland, where fine lenses host paleo seawater.

2. In GP, the areas with the highest probability of exceeding the NO_3^- threshold are in specific hotspots in the middle of the plain. As for Cl^-, the highest probabilities are near the Garigliano River mouth and in a small area in the centre of the plain.
3. In HVP, only the NO_3^- probability map is presented since the selected cutoff value for Cl^- (90 mg/L) was never reached. For NO_3^-, the probability increases from south to north, but decreases in the eastern and central parts.
4. The results obtained using DT, RF, and IGR showed that in all areas the parameters having the greatest effect on NO_3^- pollution are recharge and hydraulic conductivity.
5. The results of the three algorithms showed that in LVP and GP, the parameters that have the greatest effect on Cl^- salinization are recharge and distance from the superficial bodies.
6. The findings indicate an elevated level of reliability of the SGS results, with a correlation coefficient of 0.97 for NO_3^- and 0.67 for Cl^-.

In conclusion, due to the different processes governing NO_3^- pollution and Cl^- salinization in different areas of the Campania Region characterized by different hydrogeological and socio-economic drivers, an informed management is essential to effectively tackle protection measures to safeguard groundwater resources. The approach presented in this study can be extended to other regions, helping policymakers and managers to identify areas exposed to potential human and naturally driven pollution, since the framework was tested in three study areas (well-documented areas, with similarities and differences) and the obtained results are consistent with the previous knowledge.

Supplementary Information The online version contains supplementary material available at https://doi.org/10.1007/s11069-025-07300-5.

Acknowledgements The authors would like to thank the European Commission and MUR for funding this research in the frame of the collaborative international consortium DATASET (Groundwater salinization and pollution assessment tool: a holistic approach for coastal areas, Water4All_00084), financed under the 2022 Joint call of the European Partnership 101060874 - Water4All. Dr. Stefania Stevenazzi also acknowledges the Italian Ministry of Education, University and Research in the framework of the National Operational Programme Research & Innovation 2014–2020 - Axis IV, "Education and research for recovery - REACT-EU" (Università degli Studi di Napoli Federico II: CUP E65F21003160003).

Author contributions The authors Micòl Mastrocicco, Gianluigi Busico and Mojgan Bordbar contributed to the study conception and design. Material preparation, data collection and analysis were performed by Mojgan Bordbar, Gianluigi Busico. The first draft of the manuscript was written by Mojgan Bordbar and revised by Stefania Stevenazzi, Gianluigi Busico and Micòl Mastrocicco. All authors read and approved the final manuscript.

Funding Open access funding provided by Università degli Studi della Campania Luigi Vanvitelli within the CRUI-CARE Agreement.
This work was supported by the 2022 Joint call of the European Partnership 101060874 (Grant numbers Water4All_00084).

Data availability All data and materials are available upon request to the corresponding author.

Declarations

Competing interests The authors have no relevant financial or non-financial interests to disclose.

References

Abbaspour KC, Vaghefi SA, Yang H, Srinivasan R (2019) Global soil, land use, evapotranspiration, historical and future weather databases for SWAT applications. Sci Data 6(1):263. https://doi.org/10.1038/s41597-019-0282-4

Adhikary PP, Dash CJ, Bej R, Chandrasekharan H (2011) Indicator and probability kriging methods for delineating Cu, Fe, and Mn contamination in groundwater of Najafgarh block, Delhi, India. Environ Monit Assess 176:663–676. https://doi.org/10.1007/s10661-010-1611-4

Akbulut Özen S, Yesilkanat CM, Özen M, Başsarı A, Taşkın H (2022) Health risk assessment of soil trace elements using the sequential Gaussian simulation approach. Environ Sci Pollut Res 29(48):72683–72698. https://doi.org/10.1007/s11356-022-20974-9

Allocca V, Celico F, Celico P, De Vita P, Fabbrocino S, Mattia C, Monacelli G, Musilli I, Piscopo V, Scalise AR, Summa G, Tranfaglia G (2007) Carta Idrogeologica dell'Italia Meridionale. Istituto Poligrafico e Zecca dello Stato

Aryafar A, Khosravi V, Karami S (2020) Groundwater quality assessment of Birjand plain aquifer using kriging Estimation and sequential Gaussian simulation methods. Environ Earth Sci 79:1–21. https://doi.org/10.1007/s12665-020-08905-8

Ascott MJ, Gooddy DC, Wang L, Stuart ME et al (2017) Global patterns of nitrate storage in the vadose zone. Nat Commun 8(1):1416. https://doi.org/10.1038/s41467-017-01321

Bai T, Tahmasebi P (2022) Sequential Gaussian simulation for geosystems modeling: a machine learning approach. Geosci Front 13(1):101258. https://doi.org/10.1016/j.gsf.2021.101258

Bajni G, Camera CAS, Apuani T (2023) A novel dynamic rockfall susceptibility model including precipitation, temperature and snowmelt predictors: a case study in Aosta Valley (northern Italy). Landslides 20:2131–2154. https://doi.org/10.1007/s10346-023-02091-x

Balacco G, Fiorese GD, Alfio MR (2023) Assessment of groundwater nitrate pollution using the Indicator kriging approach. Groundw Sustain Dev 21:100920. https://doi.org/10.1016/j.gsd.2023.100920

Batjes NH, Ribeiro E, Van Oostrum A et al (2017) WoSIS: providing standardised soil profile data for the world. Earth Syst Sci Data 9(1):1–14. https://doi.org/10.5194/essd-9-1-2017

Bodrud-Doza M, Bhuiyan MAH, Islam SDU et al (2019) Delineation of trace metals contamination in groundwater using Geostatistical techniques: A study on Dhaka City of Bangladesh. Groundw Sustain Dev 9:100212. https://doi.org/10.1016/j.gsd.2019.03.006

Bordbar M, Aghamohammadi H, Pourghasemi HR, Azizi Z (2022) Multi-hazard Spatial modeling via ensembles of machine learning and meta-heuristic techniques. Sci Rep 12(1):1451. https://doi.org/10.1038/s41598-022-05364-y

Bordbar M, Busico G, Sirna M, Tedesco D, Mastrocicco M (2023a) A multi-step approach to evaluate the sustainable use of groundwater resources for human consumption and agriculture. J Environ Manage 347:119041. https://doi.org/10.1016/j.jenvman.2023.119041

Bordbar M, Nikoo MR, Sana A et al (2023b) Assessment of the vulnerability of hybrid coastal aquifers: application of multi-attribute decision-making and optimization models. Hydrol Sci J 68(8):1095–1108. https://doi.org/10.1080/02626667.2023.2203825

Boufekane A, Maizi D, Madene E, Busico G, Zghibi A (2022) Hybridization of GALDIT method to assess actual and future coastal vulnerability to seawater intrusion. J Environ Manage 318:115580. https://doi.org/10.1016/j.jenvman.2022.115580

Bouhout S, Haboubi K, Zian A, Elyoubi MS, Elabdouni A (2022) Evaluation of two linear kriging methods for piezometric levels interpolation and a framework for upgrading groundwater level monitoring network in Ghiss-Nekor plain, north-eastern Morocco. Arab J Geosci 15(10):1016. https://doi.org/10.1007/s12517-022-10283-3

Busico G, Cuoco E, Kazakis N, Colombani N et al (2018) Multivariate statistical analysis to characterize/discriminate between anthropogenic and Geogenic trace elements occurrence in the campania plain, Southern Italy. Environ Pollut 234:260–269. https://doi.org/10.1016/j.envpol.2017.11.053

Busico G, Kazakis N, Cuoco E et al (2020) A novel hybrid method of specific vulnerability to anthropogenic pollution using multivariate statistical and regression analyses. Water Res 171:115386. https://doi.org/10.1016/j.watres.2019.115386

Busico G, Buffardi C, Ntona MM, Vigliotti M, Colombani N, Mastrocicco M, Ruberti D (2021) Actual and forecasted vulnerability assessment to seawater intrusion via GALDIT-SUSI in the Volturno river mouth (Italy). Remote Sens 13(18):3632. https://doi.org/10.3390/rs13183632

Busico G, Bordbar M, Rufino F, Sarracino A, Tedesco D (2024) Assessment of NO_3^-, as, and F^- background levels in groundwater bodies: A methodological review and case study utilizing sequential Gaussian simulation (SGS). https://doi.org/10.1016/j.gsd.2024.101211. Groundw Sustain Dev 26

Candra IN, Gerzabek MH, Ottner F et al (2023) Soil formation and mineralogical changes on basaltic lava vs scoria along a hydroclimatic gradient on Santa Cruz Island, Galápagos. Catena 220 https://doi.org/10.1016/j.catena.2022.106696

Chica-Olmo M, Luque-Espinar JA, Rodriguez-Galiano V, Pardo-Igúzquiza E, Chica-Rivas L (2014) Categorical Indicator kriging for assessing the risk of groundwater nitrate pollution: the case of Vega de Granada aquifer (SE Spain). Sci Tot Environ 470–471. https://doi.org/10.1016/J.SCITOTENV.2013.09.077

Chowdhuri I, Pal SC, Chakrabortty R, Malik S, Das B, Roy P (2021) Torrential rainfall-induced landslide susceptibility assessment using machine learning and statistical methods of Eastern himalaya. Nat Hazards 107:697–722. https://doi.org/10.1007/s11069-021-04601-3

Cinnirella S, Buttafuoco G, Pirrone N (2005) Stochastic analysis to assess the Spatial distribution of groundwater nitrate concentrations in the Po catchment (Italy). Environ Pollut 133(3):569–580. https://doi.org/10.1016/j.envpol.2004.06.020

De Vita P, Allocca V, Celico F et al (2018) Hydrogeology of continental Southern Italy. J Maps 14:230–241. https://doi.org/10.1080/17445647.2018.1454352

Ducci D, Sellerino M (2013) Vulnerability mapping of groundwater contamination based on 3D lithostratigraphical models of porous aquifers. Sci Tot Environ 447:315–322. https://doi.org/10.1016/j.scitotenv.2012.12.090

Ducci D, de Melo MTC, Preziosi E, Sellerino M, Parrone D, Ribeiro L (2016) Combining natural background levels (NBLs) assessment with indicator kriging analysis to improve groundwater quality data interpretation and management. Sci Total Environ 569:569–584. https://doi.org/10.1016/j.scitotenv.2016.06.184

Ez-Zaouy Y, Bouchaou L, Schreiber H et al (2023) Combined geophysical methods to investigate seawater intrusion in the Souss-Massa coastal area, Morocco. Groundw Sustain Dev 21:100915. https://doi.org/10.1016/j.gsd.2023.100915

Gaiolini M, Colombani N, Mastrocicco M, Postacchini M (2023) Seawater intrusion assessment along the Volturno river (Italy) via numerical modeling and spectral analysis. J Hydrol 626:130289. https://doi.org/10.1016/j.jhydrol.2023.130289

Gleeson T, Cuthbert M, Ferguson G, Perrone D (2020) Global groundwater sustainability, resources, and systems in the anthropocene. Annu Rev Earth Planet Sci 48:431–463. https://doi.org/10.1146/annurev-earth-071719-055251

Islam ARMT, Ahmed N, Bodrud-Doza M, Chu R (2017) Characterizing groundwater quality ranks for drinking purposes in Sylhet district, Bangladesh, using entropy method, Spatial autocorrelation index, and geostatistics. Environ Sci Pollut Res 24:26350–26374. https://doi.org/10.1007/s11356-017-0254-1

Karami S, Jalali M, Karami A, Katibeh H, Marj AF (2022) Evaluating and modeling the groundwater in Hamedan plain aquifer, Iran, using the linear Geostatistical estimation, sequential Gaussian simulation, and turning band simulation approaches. Model Earth Syst Environ 8:3555–3357. https://doi.org/10.1007/s40808-021-01295-1

Khan M, Almazah MM, EIlahi A, Niaz R, Al-Rezami AY, Zaman B (2023) Spatial interpolation of water quality index based on ordinary kriging and universal kriging. Geomatics Nat Hazards Risk 14(1):2190853. https://doi.org/10.1080/19475705.2023.2190853

Khosravi K, Sartaj M, Tsai FTC et al (2018) A comparison study of DRASTIC methods with various objective methods for groundwater vulnerability assessment. Sci Total Environ 642:1032–1049. https://doi.org/10.1016/j.scitotenv.2018.06.130

Khosravi K, Bordbar M, Paryani S, Saco PM, Kazakis N (2021) New hybrid-based approach for improving the accuracy of coastal aquifer vulnerability assessment maps. Sci Total Environ 767:145416. https://doi.org/10.1016/j.scitotenv.2021.145416

Li J, Li X, Lv N et al (2015) Quantitative assessment of groundwater pollution intensity on typical contaminated sites in China using grey relational analysis and numerical simulation. Environ Earth Sci 74:3955–3968. https://doi.org/10.1007/s12665-014-3980-4

Li J, Yu S, Liu Q et al (2023) Screening of hazardous groundwater pollutants responsible for microbial ecological consequences by integrated nontargeted analysis and high-throughput sequencing technologies. J Hazard Mater 445:130516. https://doi.org/10.1016/j.jhazmat.2022.130516

Luo S, Xu L, Yu J, Zhou W, Yang Z, Wang S, Shu Q (2023) Sampling Estimation and optimization of typical forest biomass based on sequential Gaussian conditional simulation. Forests 14(9):1792. https://doi.org/10.3390/f14091792

Lv J, Wang Y (2019) PMF receptor models and sequential Gaussian simulation to determine the quantitative sources and hazardous areas of potentially toxic elements in soils. Geoderma 353:347–358. https://doi.org/10.1016/J.GEODERMA.2019.07.020

Ma R, Zhu X, Tian Z, Qu L, He Y, Liang Y (2022) Spatial distribution and scale-specific controls of soil water-stable aggregates in southeastern China. J Clean Prod 369:133305. https://doi.org/10.1016/j.jclepro.2022.133305

Machiwal D, Jha MK, Singh VP, Mohan C (2018) Assessment and mapping of groundwater vulnerability to pollution: current status and challenges. Earth Sci Rev 185:901–927. https://doi.org/10.1016/j.earscirev.2018.08.009

Malagó A, Bouraoui F (2021) Global anthropogenic and natural nutrient fluxes: from local to planetary assessments. Environ Res Let 16(5). https://doi.org/10.1088/1748-9326/abe95f

Mastrocicco M, Giambastiani BMS, Colombani N (2013) Ammonium occurrence in a salinized lowland coastal aquifer (Ferrara, Italy). Hydrol Process 27(24):3495–3501. https://doi.org/10.1002/hyp.9467

Mastrocicco M, Gervasio MP, Busico G, Colombani N (2021) Natural and anthropogenic factors driving groundwater resources salinization for agriculture use in the campania plains (Southern Italy). Sci Total Environ 758:144033. https://doi.org/10.1016/j.scitotenv.2020.144033

Misstear B, Banks D, Clark L (2006) Appendix 3 FAO irrigation water quality guidelines. Chichester: water wells and boreholes. John Wiley & Sons, Ltd.

Nussbaumer R, Mariethoz G, Gravey M, Gloaguen E, Holliger K (2018) Accelerating sequential Gaussian simulation with a constant path. Comput Geosci 112:121–132. https://doi.org/10.1016/j.cageo.2017.12.006

Ouarani M, Brahim YA, Mulla D, Rafik A, Azennoud K, Bouchaou L, Chehbouni A (2023) A comprehensive overview of groundwater salinization and recharge processes in a semi-arid coastal aquifer (Essaouira, Morocco). J Hydrol Reg Stud 49:101501. https://doi.org/10.1016/j.ejrh.2023.101501

Poggio L, De Sousa LM, Batjes NH et al (2021) SoilGrids 2.0: producing soil information for the Globe with quantified Spatial uncertainty. Soil 7(1):217–240. https://doi.org/10.5194/soil-7-217-2021

Pourghasemi HR, Pouyan S, Bordbar M, Golkar F, Clague JJ (2023) Flood, landslides, forest fire, and earthquake susceptibility maps using machine learning techniques and their combination. Nat Hazards 116(3):3797–3816. https://doi.org/10.1007/s11069-023-05836-y

Rama F, Busico G, Arumi JL et al (2022) Assessment of intrinsic aquifer vulnerability at continental scale through a critical application of the drastic framework: the case of South America. Sci Total Environ 823:153748. https://doi.org/10.1016/j.scitotenv.2022.153748

Rufino F, Busico G, Cuoco E, Darrah TH, Tedesco D (2019) Evaluating the suitability of urban groundwater resources for drinking water and irrigation purposes: an integrated approach in the Agro-Aversano area of Southern Italy. Environ Monit Assess 191:1–17. https://doi.org/10.1007/s10661-019-7978-y

Schiavo M, Colombani N, Mastrocicco M (2023) Modeling stochastic saline groundwater occurrence in coastal aquifers. Water Res 235:119885. https://doi.org/10.1016/j.watres.2023.119885

Stevenazzi S, Bonfanti M, Masetti M, Nghiem SV, Sorichetta A (2017) A versatile method for groundwater vulnerability projections in future scenarios. J Environ Manag 187:365–374. https://doi.org/10.1016/j.jenvman.2016.10.057

Sun H, Hu X (2017) Attribute selection for decision tree learning with class constraint. Chemom Intell Lab Syst 163:16–23. https://doi.org/10.1016/j.chemolab.2017.02.004

Taghavi N, Niven RK, Paull DJ, Kramer M (2022) Groundwater vulnerability assessment: A review including new statistical and hybrid methods. Sci Total Environ 822:153486. https://doi.org/10.1016/j.scitotenv.2022.153486

Wang Z, Lu W, Chang Z, Luo J (2023) A combined search method based on a deep learning combined surrogate model for groundwater DNAPL contamination source identification. J Hydrol 616:128854. https://doi.org/10.1016/j.jhydrol.2022.128854

WHO: World Health Organization (2017) Guidelines for drinking-water quality: first addendum to the fourth edition. ISBN: 978-92-4-154995-0

Xu H, Yang X, Wang D et al (2023) Multivariate and spatio-temporal groundwater pollution risk assessment: A new long-time serial groundwater environmental impact assessment system. Environ Pollut 317:120621. https://doi.org/10.1016/j.envpol.2022.120621

Zeng X, Wu J, Wang D, Zhu X (2016) Assessing the pollution risk of a groundwater source field at Western Laizhou Bay under seawater intrusion. Environ Res 148:586–594. https://doi.org/10.1016/j.envres.2015.11.022

Matano F, Sacchi M, Vigliotti M, Ruberti D (2018) Subsidence trends of Volturno River Coastal Plain (Northern Campania, Southern Italy) inferred by SAR Interferometry Data. Geosciences 8(1):8. https://doi.org/10.3390/geosciences8010008

Authors and Affiliations

Mojgan Bordbar[1] · Gianluigi Busico[1] · Stefania Stevenazzi[2] · Micòl Mastrocicco[1]

✉ Gianluigi Busico
gianluigi.busico@unicampania.it

1 Department of Environmental, Biological and Pharmaceutical Sciences and Technologies (DiSTABiF), Campania University "Luigi Vanvitelli", Via A. Vivaldi 43, Caserta 81100, Italy

2 Department of Civil, Building and Environmental Engineering, University of Naples Federico II, Piazzale Tecchio 80, Naples 80125, Italy